M-SFDA: Meta Network with Spatial Interaction for Source-Free Domain Adaptation in Prostate MRI Segmentation using Segment Anything Model

Yihang Fu[1⋆], Ziyang Chen[1⋆], Rongze Ma[1], and Yong Xia[1,2,3(✉)]

[1] National Engineering Laboratory for Integrated Aero-Space-Ground-Ocean Big Data Application Technology, School of Computer Science and Engineering, Northwestern Polytechnical University, Xi'an 710072, China
[2] Ningbo Institute of Northwestern Polytechnical University, Ningbo 315048, China
[3] Research & Development Institute of Northwestern Polytechnical University in Shenzhen, Shenzhen 518057, China
yihang.fu@mail.nwpu.edu.cn, zychen@mail.nwpu.edu.cn, rongzema129@mail.nwpu.edu.cn, yxia@nwpu.edu.cn

Abstract. Domain shift caused by heterogeneous scanners and imaging protocols remains a major obstacle to deploying medical image segmentation models across clinical centres. Source-free domain adaptation (SFDA) addresses this challenge by adapting a source-trained model to unlabeled target samples without accessing source data, thus complying with privacy constraints. While recent SFDA methods rely primarily on pseudo-label refinement or entropy minimization, directly optimizing large-scale foundation models under noisy self-training signals often leads to limited generalization and unstable convergence. In this work, we propose a meta-spatial adaptation framework built upon the Segment Anything Model (SAM) for prostate MRI segmentation, termed M-SFDA. Instead of updating the entire model, we introduce meta networks into the SAM's image encoder to enable input-adaptive feature refinement. These meta networks explicitly model bidirectional spatial interactions along height and width axes, compensating for the limited spatial inductive bias of patch-based transformers. To further stabilize adaptation under unreliable pseudo supervision, we incorporate sharpness-aware optimization to encourage flatter minima and improve generalization. Extensive experiments on a six-domain prostate MRI benchmark demonstrate that M-SFDA consistently outperforms state-of-the-art SFDA approaches and achieves superior average Dice scores across diverse cross-domain scenarios. Our results highlight the potential of spatially adaptive strategies for medical foundation models under source-free settings.

Keywords: Source-free domain adaptation · Segment anything model · Prostate MRI segmentation

⋆ Y. Fu and Z. Chen contributed equally. Corresponding author: Y. Xia.

1 Introduction

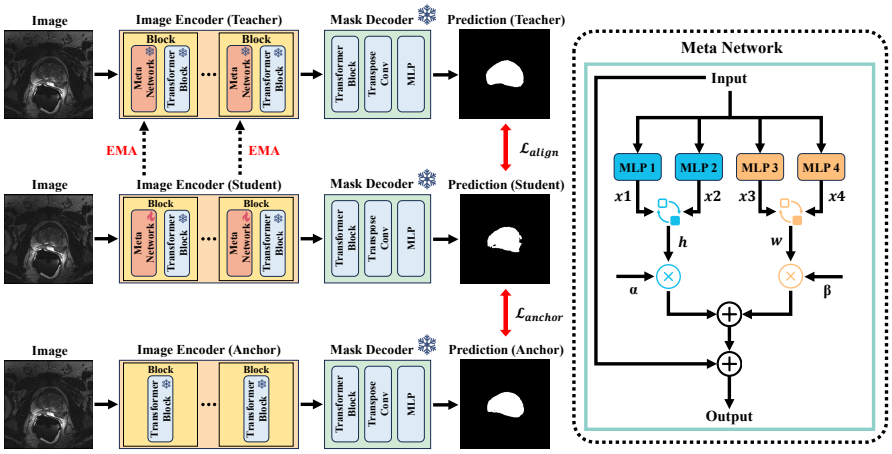

Fig. 1. Overview of our proposed M-SFDA and the meta network. Our M-SFDA is based on a traditional teacher-student framework with an exponential moving average (EMA) strategy. By integrating meta networks with bidirectional spatial interactions into SAM, we enable it to adaptively leverage input to perform feature refinement.

Deep learning has substantially advanced medical image segmentation [1], particularly with the emergence of large-scale vision transformers and foundation models. Nevertheless, segmentation models trained on labeled data from a specific centre (source domain) often suffer notable performance degradation when deployed to new hospitals (target domains). Such degradation is primarily caused by domain shift arising from variations in scanners, acquisition protocols, and patient populations [24,25,12].

Unsupervised domain adaptation (UDA) has been extensively studied to alleviate domain shift by leveraging both labeled source data and unlabeled target data [27,8,16,5,4,13,9]. However, in real-world clinical scenarios, source data are frequently inaccessible due to privacy regulations and institutional restrictions. This limitation has motivated increasing attention toward source-free domain adaptation (SFDA), where adaptation must be performed using only a pre-trained source model and unlabeled target samples.

Existing SFDA approaches for medical image segmentation can be broadly categorized into data-driven and model-driven paradigms. Data-driven methods attempt to reconstruct or approximate the missing source distribution, for example by separating target data into pseudo source/target subsets [23,6]. Their effectiveness, however, heavily depends on the quality of the reconstructed distribution, which is difficult to guarantee in practice. Model-driven approaches

instead rely on self-training strategies such as pseudo-label denoising [2,26], entropy minimization [18], or prompt learning [14]. Although more practical, these methods face two intrinsic challenges: (1) unreliable pseudo supervision may bias optimization toward incorrect target structures, and (2) directly fine-tuning large-scale foundation models can result in unstable training and convergence to sharp minima, ultimately limiting cross-domain generalization.

Meanwhile, foundation models such as the Segment Anything Model [17] (SAM) have demonstrated remarkable generalization across natural images and have recently been adapted to medical segmentation tasks. However, SAM adopts a patch-based transformer encoder with limited explicit spatial inductive bias. When confronted with cross-centre MRI variations, naïvely adapting the entire encoder in a source-free manner is prone to overfitting noisy pseudo-labels.

To address these challenges, we propose **M-SFDA**, a meta-spatial adaptation framework for SAM under the source-free setting. Instead of updating the full backbone, we introduce meta networks into selected blocks of the SAM's image encoder. These meta networks perform bidirectional spatial interaction along both height and width axes, capturing long-range row–column dependencies and enriching spatial representations that are otherwise weakened by patch tokenization. Importantly, the meta networks act as input-adaptive feature modulators, enabling targeted adaptation to the target domain. To further enhance adaptation stability, we incorporate sharpness-aware optimization [10] during the training process of meta networks. By explicitly seeking flatter minima in the parameter landscape, the model becomes less sensitive to noisy pseudo-labels and better generalizes to the target distribution. We validate the proposed method on a multi-centre prostate T2-weighted MRI benchmark comprising six domains, covering diverse cross-domain adaptation scenarios. Extensive experiments demonstrate that M-SFDA consistently achieves superior average Dice scores compared with strong SFDA baselines.

Our contributions are three-fold. (1) We propose a meta-spatial adaptation strategy for SAM that introduces meta networks with bidirectional spatial interactions for input-adaptive feature refinement under SFDA. (2) We integrate sharpness-aware optimization into the source-free self-training process to promote flatter minima and stabilize adaptation. (3) We demonstrate state-of-the-art performance on multi-domain prostate MRI segmentation, validating the effectiveness of spatially adaptive and stability-aware adaptation for medical foundation models.

2 Methodology

2.1 Overview

We define the source domain $\mathcal{D}^s = \{(x_i^s, y_i^s)\}_{i=1}^{N_s}$, where x_i^s is the i-th image in the source domain, y_i^s is its corresponding label, and N_s is the number of samples. Given a model $f^s : x^s \to y^s$ pre-trained on $\mathcal{D}^s$, source-free domain adaptation aims at acquiring a target-adapted model $f^t : x^t \to y^t$ by leveraging

the source-trained model f^s in conjunction with unlabeled target data $\mathcal{D}^t = \{x_i^t\}_{i=1}^{N_t}$ without accessing any source data.

An overview of our M-SFDA is illustrated in Fig. 1. Our M-SFDA is based on a traditional teacher-student framework using a consistency loss $\mathcal{L}_{align} = \mathcal{L}_{seg}(f_{stu}^t(x^t), f_{tea}^t(x^t))$ with an exponential moving average (EMA) strategy controlled by momentum η, where f_{stu}^t and f_{tea}^t denote the student model and teacher model, respectively. The meta networks are incorporated into the blocks of the SAM's image encoder. Additionally, we introduce the original pre-trained model f^s to construct an anchor loss $\mathcal{L}_{anchor} = \mathcal{L}_{seg}(f_{stu}^t(x^t), f^s(x^t))$, preventing catastrophic forgetting during the adaptation process. The basic segmentation loss $\mathcal{L}_{seg}$ is the combination of Dice loss and cross-entropy loss. We construct a multi-task loss $\mathcal{L} = \mathcal{L}_{align} + \mathcal{L}_{anchor}$ and introduce the sharpness-aware optimization to update the parameters of our meta networks. We utilize image-sized bounding boxes as prompts, omitting the SAM's prompt encoder for simplicity. We now delve into the details.

2.2 Meta Network

Algorithm 1 PyTorch-like pseudo-code of the meta network.

```
# x: input feature (B, H, W, C)
# MLP1, MLP2, MLP3, MLP4: four MLPs (Linear - ReLU - Linear - LayerNorm)
# g(): sigmoid function; interpolate(): interpolation operator
# α, β: learnable parameters initialized with g(-5) (1, 1, 1, C)

# 1. Obtain latent features
x1 = MLP1(x)  # (B, H, W, C)
x2 = MLP2(x)  # (B, H, W, C)
x3 = MLP3(x)  # (B, H, W, C)
x4 = MLP4(x)  # (B, H, W, C)

# 2. Perform bidirectional spatial interactions
x1 = x1.permute(0, 3, 1, 2)  # (B, C, H, W)
x2 = x2.permute(0, 3, 2, 1)  # (B, C, W, H)
h = torch.matmul(x1, x2).permute(0, 2, 3, 1)  # (B, H, H, C)

x3 = x3.permute(0, 3, 2, 1)  # (B, C, W, H)
x4 = x4.permute(0, 3, 1, 2)  # (B, C, H, W)
w = torch.matmul(x3, x4).permute(0, 2, 3, 1)  # (B, W, W, C)

# 3. Supplement spatial information adaptively
return x + g(α) * interpolate(h) + g(β) * interpolate(w)
```

As shown in Algorithm 1, we represent input features as $x \in \mathbb{R}^{B\times H\times W\times C}$, where B, C, H and W denote the batch size, the feature dimension, the height

and width of the features, respectively. We first pass x through four multi-layer perceptrons (MLP) to obtain latent features. Then, we perform matrix multiplication along the height and width directions. The interaction matrices $h \in \mathbb{R}^{B\times H\times H\times C}$ and $w \in \mathbb{R}^{B\times W\times W\times C}$ can capture the spatial correlation between row and column feature vectors, respectively. Subsequently, we introduce learnable adaptive weights α and β, which assist in supplementing the spatial interaction information to the original input. To adapt to the input, we apply interpolation on h and w to obtain the output. We incorporate the meta network into the SAM's image encoder, specifically before the first M blocks.

2.3 Sharpness-aware Optimization

The conventional objective optimizes the parameters of meta networks θ_m by minimizing the loss $\mathcal{L}(\theta_m)$. However, in SFDA, unreliable training signals often drive the optimization toward sharp minima, resulting in unstable adaptation and suboptimal generalization performance. To mitigate this issue, we introduce the sharpness-aware optimization, which seeks parameters θ_m that jointly minimize both the loss value and the local curvature, thereby promoting flatter minima and improving adaptation stability. It can be formulated as:

$$\min_{\theta_m} \mathcal{L}^{Sharpness}(\theta_m) + \lambda\|\theta_m\|_2^2, \quad \mathcal{L}^{Sharpness}(\theta_m) \triangleq \max_{\|\boldsymbol{\epsilon}\|_2\leq\rho} \mathcal{L}(\theta_m + \boldsymbol{\epsilon}), \tag{1}$$

where ρ denotes the neighborhood size, and λ controls the strength of the regularization term. Following [10], we solve the inner optimization via first-order Taylor expansion, obtaining

$$\begin{aligned} \boldsymbol{\epsilon}^*(\theta_m) = \arg\max_{\|\boldsymbol{\epsilon}\|_2\leq\rho} \mathcal{L}(\theta_m + \boldsymbol{\epsilon}) &\approx \arg\max_{\|\boldsymbol{\epsilon}\|_2\leq\rho} \mathcal{L}(\theta_m) + \boldsymbol{\epsilon}^{\mathsf{T}}\nabla_{\theta_m}\mathcal{L}(\theta_m) \\ &= \arg\max_{\|\boldsymbol{\epsilon}\|_2\leq\rho} \boldsymbol{\epsilon}^{\mathsf{T}}\nabla_{\theta_m}\mathcal{L}(\theta_m). \end{aligned} \tag{2}$$

Then, the value $\hat{\boldsymbol{\epsilon}}(\theta_m)$ to solve this approximation is given by the solution to a classical dual norm problem, defined as:

$$\hat{\boldsymbol{\epsilon}}(\theta_m) = \rho\,\mathrm{sign}\left(\nabla_{\theta_m}\mathcal{L}(\theta_m)\right)\left|\nabla_{\theta_m}\mathcal{L}(\theta_m)\right| / \left(\|\nabla_{\theta_m}\mathcal{L}(\theta_m)\|_2^2\right)^{1/2}. \tag{3}$$

To further accelerate the computation, the second-order term is omitted, and the final gradient approximation can be denoted as:

$$\nabla_{\theta_m}\mathcal{L}^{Sharpness}(\theta_m) \approx \nabla_{\theta_m}\mathcal{L}(\theta_m)\big|_{\theta_m+\hat{\boldsymbol{\epsilon}}(\theta_m)}. \tag{4}$$

3 Experiments

3.1 Datasets and Metrics

We evaluated M-SFDA on the prostate segmentation benchmark task. We used T2-weighted MRI data collected from six different data sources: Domain A

(RUNMC), Domain B (BMC), Domain C (HCRUDB), Domain D (UCL), Domain E (BIDMC), and Domain F (HK). Each domain possesses 30, 30, 19, 13, 12, and 12 3D volumes, respectively [22]. Following [15,3], we preprocessed all the cases by retaining only the 2D slices containing the prostate region, ensuring consistent and objective segmentation evaluation. These 2D slices were resized to 384×384 while maintaining the same voxel spacing. All datasets were randomly divided into training and testing sets in a 4:1 ratio. We used the Dice similarity coefficient (DSC) as the evaluation metric. Note that this task is formulated as a 2D segmentation task, but the metric is calculated on 3D volumes. We adopt each domain as the source domain and each of remaining domains as the target domain to conduct diverse SFDA scenarios. The average performance across all remaining domains is displayed for evaluation.

3.2 Implementation Details

Following [11], we obtained the source model by training the original SAM with ViT-B [7] as the backbone using the Adam optimizer for 100 epochs. The initial learning rate η_0 was set to 1E-4, and the learning rate for each epoch was computed according to $\eta_t = \eta_0 \times (1 - \frac{t}{T})^{0.9}$, where t is the current epoch and T is the total number of epochs. The batch size was set to 16. During the source-free domain adaptation process, we set the batch size and total epochs to 8 and 10. The number of meta networks in the image encoder M, EMA coefficient η, and neighborhood size ρ in the optimizer were set to 12, 0.95 and 0.05, respectively.

Table 1. Performance of our M-SFDA, Source-Only, Target-Only, and five competing methods on the prostate segmentation task. The best and second-best results in each column are highlighted in **bold** and underline, respectively.

Methods	Domain A	Domain B	Domain C	Domain D	Domain E	Domain F	Average
	DSC	*DSC*	*DSC*	*DSC*	*DSC*	*DSC*	*DSC* ↑
Source-Only (Lower Bound)	72.16	79.54	56.36	59.90	70.34	61.81	66.68
Target-Only (Upper Bound)	90.51	87.91	83.86	88.26	87.14	86.15	87.31
DPL [2]	73.63	<u>80.43</u>	58.01	63.39	74.39	62.61	68.74
PETS [21]	74.53	80.35	<u>63.41</u>	<u>63.52</u>	76.16	62.30	<u>70.04</u>
UPL-SFDA [26]	76.86	74.57	**64.08**	58.24	<u>77.85</u>	**68.14**	69.96
PLPB [20]	73.21	<u>80.43</u>	59.64	58.08	71.88	66.26	68.25
AIF-SFDA [19]	**77.95**	77.71	60.84	**63.79**	71.65	65.24	69.53
M-SFDA (Ours)	<u>77.78</u>	**83.04**	60.41	60.86	**78.76**	<u>67.33</u>	**71.36**

3.3 Results

Comparison on the prostate segmentation task. We compared our M-SFDA with Source-Only (the model is directly used for inference without adaptation), Target-Only (the model is trained with labeled target domain images), and five competing SFDA methods, including: (1) A method based on denoised

Table 2. Performance of different component combinations on the prostate segmentation task. The best and second-best results in each column are highlighted in **bold** and underline, respectively.

Combinations		Domain A	Domain B	Domain C	Domain D	Domain E	Domain F	Average
Meta Network	$\mathcal{L}^{Sharpness}$	*DSC*	*DSC*	*DSC*	*DSC*	*DSC*	*DSC*	*DSC* ↑
		72.16	79.54	56.36	59.90	70.34	61.81	66.68
✓		**79.21**	81.94	58.63	59.29	78.47	65.48	70.50
✓	✓	77.78	**83.04**	**60.41**	**60.86**	**78.76**	**67.33**	**71.36**

Table 3. Performance of different architectures of the meta network on the prostate segmentation task. The best and second-best results in each column are highlighted in **bold** and underline, respectively.

Architecture	Domain A	Domain B	Domain C	Domain D	Domain E	Domain F	Average
	DSC	*DSC*	*DSC*	*DSC*	*DSC*	*DSC*	*DSC* ↑
Source-Only	72.16	79.54	56.36	59.90	70.34	61.81	66.68
MLP	77.64	81.53	43.17	59.58	77.00	65.78	67.45
Convolution	75.48	79.10	58.23	59.96	77.26	65.10	69.19
Attention	75.47	77.46	59.63	59.24	77.12	65.66	69.10
M-SFDA (Ours)	**77.78**	**83.04**	**60.41**	**60.86**	**78.76**	**67.33**	**71.36**

Table 4. Performance of different spatial interaction combinations on the prostate segmentation task. The best and second-best results in each column are highlighted in **bold** and underline, respectively.

Combinations		Domain A	Domain B	Domain C	Domain D	Domain E	Domain F	Average
height-axis	width-axis	*DSC*	*DSC*	*DSC*	*DSC*	*DSC*	*DSC*	*DSC* ↑
		72.16	79.54	56.36	59.90	70.34	61.81	66.68
✓		76.97	81.83	58.55	60.33	75.69	64.65	69.67
	✓	77.01	81.29	58.59	**61.28**	75.96	64.92	69.84
✓	✓	**77.78**	**83.04**	**60.41**	60.86	**78.76**	**67.33**	**71.36**

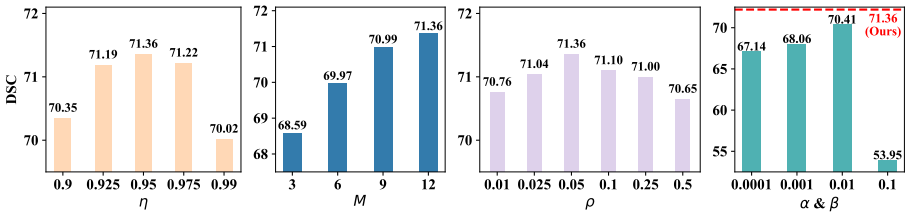

Fig. 2. Overall performance of our M-SFDA with various η, M, ρ, α and β on the prostate segmentation task.

pseudo-labeling (DPL [2]); (2) A method based on the periodically exchange teacher-student framework (PETS [21]); (3) A method based on uncertainty-aware pseudo labels (UPL-SFDA [26]); (4) A method based on robust pseudo-

labels and pseudo-boundaries (PLPB [20]); (5) A method based on autonomous information filter (AIF-SFDA [19]). As shown in Table 1, all methods outperform the Source-Only setting in average DSC, and the Target-Only setting achieves the upper bound of performance. Although our M-SFDA cannot achieve the best performance on all domains, it obtains stable gains on each domain and attains the best average performance, surpassing the second-best method (PETS) by 1.32%.

Ablation studies. We conducted ablation studies to validate the effectiveness of each component in M-SFDA on the prostate segmentation task, as shown in Table 2. The results reveal that (1) The meta network adaptively modulates features based on the input, significantly enhancing the performance across various domains. (2) The sharpness-aware optimization effectively prevents the self-training process of meta networks from converging to a sharp minimum, supporting the training process and improving average performance.

Comparison on different architectures of the meta network. In the design of the meta network, we compared several traditional architectures: (1) a single MLP identical to that used in Algorithm 1 (MLP); (2) a sequential combination of a convolutional layer, ReLU, and layer normalization (Convolution); and (3) an 8-head self-attention module (Attention). All extracted features are supplemented to the original input with adaptive weights. The results shown in Table 3 demonstrate that our spatial-interaction-based meta network achieves significant performance gains, validating its effectiveness of feature representation.

Comparison on different spatial interaction combinations. We performed experiments on the prostate segmentation task to evaluate the impact of different spatial interaction combinations. As shown in Table 4, it can be observed that: Compared to using spatial interaction in a single direction, employing bidirectional interactions integrates more spatial information, resulting in superior performance.

Analysis of hyper-parameters (η, M, and ρ) and learnable weights (α and β). We further discussed the effect of three hyper-parameters and two learnable weights on the prostate segmentation task. As shown in Fig. 2, the results indicate that: (1) The optimal hyper-parameters for η (EMA coefficient), M (the number of meta networks in the image encoder), and ρ (neighborhood size in the optimizer) are 0.95, 12, and 0.05, respectively; and (2) To compare fixed and learnable strategies for α and β, we repeated experiments using a series of fixed weights. We observed that setting α and β to 0.01 can achieve the upper bound of performance among the fixed weights (*i.e.* 70.41). In contrast, our M-SFDA adaptively learns weights in a hyperparameter-free manner and achieves a superior performance of 71.36, demonstrating the effectiveness of our adaptive learnable weights.

4 Conclusion

In this paper, we propose a meta-spatial adaptation framework designed to alleviate domain shifts for SAM, called M-SFDA. Recognizing that standard patch tokenization can weaken spatial dependencies, we introduce meta networks into the SAM's image encoder. These meta networks facilitate bidirectional spatial interactions across height and width axes, enabling input-adaptive feature modulation. To ensure stability during self-training, we integrate the sharpness-aware optimization, which seeks for a flatter minima for model parameters, ensuring both low loss and low sharpness around neighborhoods. Extensive experiment results on the prostate MRI segmentation benchmark across multiple scenarios verify the superiority of our M-SFDA over other state-of-the-art SFDA methods.

Acknowledgments. This work was supported in part by the Science and Technology Program of Haicang District of Xiamen, China, under Grant 350205Z20242013, in part by the National Natural Science Foundation of China under Grant 92470101, in part by the "Pioneer" and "Leading Goose" R&D Program of Zhejiang, China, under Grant 2025C01201(SD2), and in part by the Innovation Foundation for Doctor Dissertations of Northwestern Polytechnical University under Grant CX2025020.

Disclosure of Interests. The authors have no competing interests to declare that are relevant to the content of this article.

References

1. Azad, R., Aghdam, E.K., Rauland, A., Jia, Y., Avval, A.H., Bozorgpour, A., Karimijafarbigloo, S., Cohen, J.P., Adeli, E., Merhof, D.: Medical image segmentation review: The success of u-net. arXiv preprint arXiv:2211.14830 (2022)
2. Chen, C., Liu, Q., Jin, Y., Dou, Q., Heng, P.A.: Source-free domain adaptive fundus image segmentation with denoised pseudo-labeling. In: International Conference on Medical Image Computing and Computer-Assisted Intervention. pp. 225–235. Springer (2021)
3. Chen, Z., Pan, Y., Ye, Y., Cui, H., Xia, Y.: Treasure in distribution: A domain randomization based multi-source domain generalization for 2d medical image segmentation. In: International Conference on Medical Image Computing and Computer-Assisted Intervention. pp. 89–99. Springer (2023)
4. Chen, Z., Pan, Y., Ye, Y., Wang, Z., Xia, Y.: Trila: Triple-level alignment based unsupervised domain adaptation for joint segmentation of optic disc and optic cup. IEEE Journal of Biomedical and Health Informatics **28**(9), 5497–5508 (2024)
5. Cui, H., Li, Y., Wang, Y., Xu, D., Wu, L.M., Xia, Y.: Towards accurate cardiac mri segmentation with variational autoencoder-based unsupervised domain adaptation. IEEE Transactions on Medical Imaging **43**(8), 2924–2936 (2024)
6. Ding, Y., Sheng, L., Liang, J., Zheng, A., He, R.: Proxymix: Proxy-based mixup training with label refinery for source-free domain adaptation. Neural Networks **167**, 92–103 (2023)
7. Dosovitskiy, A.: An image is worth 16x16 words: Transformers for image recognition at scale. arXiv preprint arXiv:2010.11929 (2020)

8. Du, D., Cui, H., Li, J., Zheng, F., Xia, Y.: Cauda-mi: Cross attention-guided unsupervised domain adaptation with mutual information for cardiac mri segmentation. In: International Conference on Medical Image Computing and Computer-Assisted Intervention. pp. 46–56. Springer (2025)
9. Du, Z., Li, X., Li, F., Lu, K., Zhu, L., Li, J.: Domain-agnostic mutual prompting for unsupervised domain adaptation. In: Proceedings of the IEEE/CVF Conference on Computer Vision and Pattern Recognition. pp. 23375–23384 (2024)
10. Foret, P., Kleiner, A., Mobahi, H., Neyshabur, B.: Sharpness-aware minimization for efficiently improving generalization. arXiv preprint arXiv:2010.01412 (2020)
11. Fu, Y., Chen, Z., Ye, Y., Lei, X., Wang, Z., Xia, Y.: Cosam: Self-correcting sam for domain generalization in 2d medical image segmentation. arXiv preprint arXiv:2411.10136 (2024)
12. Ghafoorian, M., Mehrtash, A., Kapur, T., Karssemeijer, N., Marchiori, E., Pesteie, M., Guttmann, C.R., De Leeuw, F.E., Tempany, C.M., Van Ginneken, B., et al.: Transfer learning for domain adaptation in mri: Application in brain lesion segmentation. In: International Conference on Medical Image Computing and Computer-Assisted Intervention. pp. 516–524. Springer (2017)
13. Hu, S., Liao, Z., Xia, Y.: Domain specific convolution and high frequency reconstruction based unsupervised domain adaptation for medical image segmentation. In: International Conference on Medical Image Computing and Computer-Assisted Intervention. pp. 650–659. Springer (2022)
14. Hu, S., Liao, Z., Xia, Y.: Source-free domain adaptation using prompt learning for medical image segmentation. Pattern Recognition p. 112290 (2025)
15. Hu, S., Liao, Z., Zhang, J., Xia, Y.: Domain and content adaptive convolution based multi-source domain generalization for medical image segmentation. IEEE Transactions on Medical Imaging **42**(1), 233–244 (2022)
16. Kalabizadeh, H., Griffanti, L., Yeung, P.H., Namburete, A.I., Dinsdale, N.K., Kamnitsas, K.: Unsupervised domain adaptation via content alignment for hippocampus segmentation. In: Proceedings of the IEEE/CVF International Conference on Computer Vision. pp. 1093–1103 (2025)
17. Kirillov, A., Mintun, E., Ravi, N., Mao, H., Rolland, C., Gustafson, L., Xiao, T., Whitehead, S., Berg, A.C., Lo, W.Y., et al.: Segment anything. In: Proceedings of the IEEE/CVF International Conference on Computer Vision. pp. 4015–4026 (2023)
18. Kothandaraman, D., Chandra, R., Manocha, D.: Ss-sfda: Self-supervised source-free domain adaptation for road segmentation in hazardous environments. In: Proceedings of the IEEE/CVF International Conference on Computer Vision. pp. 3049–3059 (2021)
19. Li, H., Li, H., Chen, J., Zhong, R., Niu, K., Fu, H., Liu, J.: Aif-sfda: Autonomous information filter driven source-free domain adaptation for medical image segmentation. In: Proceedings of the AAAI Conference on Artificial Intelligence. vol. 39, pp. 4716–4724 (2025)
20. Li, L., Zhou, Y., Yang, G.: Robust source-free domain adaptation for fundus image segmentation. In: Proceedings of the IEEE/CVF Winter Conference on Applications of Computer Vision. pp. 7840–7849 (2024)
21. Liu, Q., Lin, L., Shen, Z., Yang, Z.: Periodically exchange teacher-student for source-free object detection. In: Proceedings of the IEEE/CVF International Conference on Computer Vision. pp. 6414–6424 (2023)
22. Liu, Q., Dou, Q., Heng, P.A.: Shape-aware meta-learning for generalizing prostate mri segmentation to unseen domains. In: International Conference on Medical Image Computing and Computer-Assisted Intervention. pp. 475–485. Springer (2020)

23. Ma, N., Bu, J., Zhang, Z., Zhou, S.: Uncertainty-guided mixup for semi-supervised domain adaptation without source data. arXiv preprint arXiv:2107.06707 (2021)
24. Quinonero-Candela, J., Sugiyama, M., Schwaighofer, A., Lawrence, N.D.: Dataset Shift in Machine Learning. Mit Press (2008)
25. Sankaranarayanan, S., Balaji, Y., Jain, A., Lim, S.N., Chellappa, R.: Learning from synthetic data: Addressing domain shift for semantic segmentation. In: Proceedings of the IEEE Conference on Computer Vision and Pattern Recognition. pp. 3752–3761 (2018)
26. Wu, J., Wang, G., Gu, R., Lu, T., Chen, Y., Zhu, W., Vercauteren, T., Ourselin, S., Zhang, S.: Upl-sfda: Uncertainty-aware pseudo label guided source-free domain adaptation for medical image segmentation. IEEE Transactions on Medical Imaging **42**(12), 3932–3943 (2023)
27. Zhang, X., Wu, Y., Angelini, E., Li, A., Guo, J., Rasmussen, J.M., O'Connor, T.G., Wadhwa, P.D., Jackowski, A.P., Li, H., et al.: Mapseg: Unified unsupervised domain adaptation for heterogeneous medical image segmentation based on 3d masked autoencoding and pseudo-labeling. In: Proceedings of the IEEE/CVF Conference on Computer Vision and Pattern Recognition. pp. 5851–5862 (2024)